JACS
JOURNAL OF THE AMERICAN CHEMICAL SOCIETY
Article
pubs.acs.org/JACS

Electrochemistry and Electrogenerated Chemiluminescence of π-Stacked Poly(fluorenemethylene) Oligomers. Multiple, Interacting Electron Transfers

Honglan Qi,[†] Jinho Chang,[†] Sameh H. Abdelwahed,[‡] Khushabu Thakur,[‡] Rajendra Rathore,*[,‡] and Allen J. Bard*[,†]

[†]Center for Electrochemistry, Department of Chemistry and Biochemistry, The University of Texas, Austin, Texas 78712, United States

[‡]Department of Chemistry, Marquette University, P.O. Box 1881, Milwaukee, Wisconsin 53201-1881, United States

Supporting Information

ABSTRACT: The electrochemistry, spectroscopy, and electrogenerated chemiluminescence (ECL) of a series of π-stacked poly(fluorenemethylene) oligomers (F*n*, *n* = 1−6) were investigated. The pendant cofacially oriented fluorene moieties are essentially in contact with each other by Van der Waals interaction promoting electronic delocalization in these species. All six compounds give successive cyclic voltammetric one-electron (1e) oxidations in 1:1 acetonitrile/benzene (MeCN/Bz), and the multiple 1e transfer properties of all these compounds were confirmed by chronoamperometric experiments with an ultramicroelectrode and digital simulations. The potentials for oxidation of the successive 1e transfers can be explained in terms of electrostatic interactions among the fluorenes. The monomer (F1) shows one irreversible wave, while F2 shows two reversible 1e waves. F3 shows only two reversible 1e oxidation waves, which is consistent with the large energy to remove a third electron because of the greater electrostatic repulsion, so the third wave is shifted toward more positive potentials. Both F4 and F5 show three reversible 1e oxidation waves, while F6 shows four reversible 1e waves. The removal of the first electron from an oligomer becomes easier as *n* increases. The stability of the radical cations also increases with *n*. The removal of consecutive electrons from F*n* can be correlated with the distance between fluorene moieties. No reduction peaks were observed except for some broad ones at ∼−3.2 V vs SCE in THF, which is consitent with the wide highest occupied molecular orbital−lowest unoccupied molecular orbital gap in these compounds (absorbance at about 300 nm). No characteristic annihilation ECL signal was observed for these compounds in 1:1 MeCN/Bz mixed solvent. However, the ECL of F6 in the presence of the coreactant $C_2O_4^{2-}$ showed a long-wavelength ECL emission that was proposed to be electrolyzed byproduct from the radical cation.

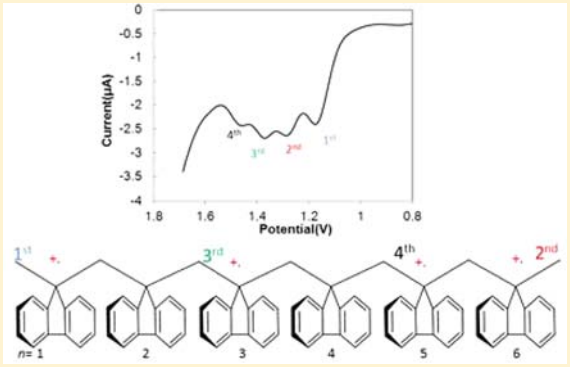

INTRODUCTION

We report here the electrochemical and photophysical characterization as well as electrogenerated chemiluminescence (ECL) of a series of π-stacked poly(fluorenemethylene) oligomers shown in Scheme 1. In these oligomers, cofacially oriented fluorene moieties are strongly interacting and have been suggested as molecular wires in possible nanoscience applications.[1−3]

The electrochemical behavior of molecules that contain two or more electroactive groups has been the subject of numerous studies. The extent of interaction between the electroactive groups in the same molecule and the rate of electron transfer between these groups affects the position, size, and shape of the electrochemical voltammetric waves. Many studies have been done on the electrochemistry of the interactions between electroactive groups on one molecule, such as polymers or dendrimers modified with ferrocenyl and other transition-metal units[4−6] and poly organic compounds.[7−11] Systems that contain two identical electroactive groups will show only a single cyclic voltammetry (CV) wave (with 1e characteristics) if the two groups do not interact.[6,11,12] However, if the groups interact strongly, they are characterized by two separate CV waves, i.e., two separate oxidation or reduction reactions, since the addition or removal of the second electron occurs with greater difficulty than that of the first.[13] The separation between the two standard potentials is quite variable, ranging from about 0.1 to over 1 V.[4] The separation is mainly dependent on the size of the molecule, the structural change associated with one or both of the electron transfers, and the degree of delocalization of the charge in the di-ion for a species with two identical electroactive groups[14] and solvation and ion pairing.[15] The resulting CV

Received: June 19, 2012
Published: September 4, 2012

   dx.doi.org/10.1021/ja3057997 | J. Am. Chem. Soc. 2012, 134, 16265−16274

Scheme 1. Chemical Structures of Various Poly(fluorenemethylene) Oligomers Examined

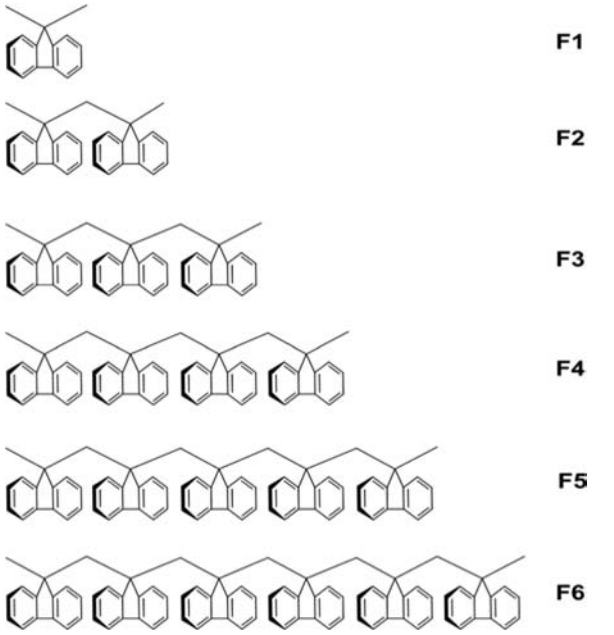

behavior for two single-electron transfers[16,17] or one two-electron process[6,11] has been discussed. Savéant et al. proposed that if the effective radius of the localized charge in the electroactive groups is smaller than the radius of the delocalized charge in the entire molecule, the net solvation energy may be larger and may induce stronger compression of the standard potentials.[17] We found, for example, that a boron dipyrromethene (BODIPY) dimer showed two 1e waves corresponding to the addition of one electron to each electroactive center of the molecule, because steric strain prevents significant electronic interaction between the electroactive groups.[7,10,18,19]

Less work has been done with multielectron transfers to a single molecule, e.g., an oligomer or polymer. For example, in the study of polyvinyl compounds, e.g., the reduction of poly(2-vinylnaphthalene), we found multielectron transfers (up to 1200 electrons per molecule) producing CV waves with the overall shape of 1e reactions; this was evidence of multiple electron transfers with no interaction between the electroactive centers on these molecules.[11] Similarly, the electrochemical oxidation of poly(vinylferrocene) also showed multielectron transfers within a single CV wave, signaling no interaction among, even Coulombic repulsion between, the pendant groups.[20] There are, in addition, a number of systems for which the removal of the second electron is significantly easier than the first, because removal of the first electron is accompanied by significant structural changes, often involving the release of steric constraints.[21,22]

Fluorene-based materials are interesting since the fluorene ring absorbs strongly in the UV region, fluoresces in the visible region, and shows good chemical and photochemical stability.[23,24] Fluorene contains a rigidly planar biphenyl unit with the C9 carbon part of the backbone rather than the fluorene acting as a pendant group. This increases the rigidity of the system and interactions among the fluorenes. Fluorene polymers have been extensively studied as electron transport materials and are promising candidates for various optoelectronic applications.[25,26] The electrochemistry and ECL of fluorene derivatives and polyfluorenes, such as ter-9,9-diarylflourenes,[27] spirobifluorene-bridged bipolar systems,[28] star-shaped truxene oligofluorenes,[23] *N*-phenylcarbazole-bridged dispirobifluorene,[29] and other fluorene derivatives,[30] have been investigated in previous studies. Most polyfluorenes have been synthesized to form cyclophanes in which the two π-systems are forced into a sandwich-like geometry that generally imparts extensive deformation of the cofacial aromatic moieties.[31] Rathore first synthesized these π-stacked molecules with multiple layers and studied electronic coupling among the cofacially oriented fluorene moieties in these multiply stacked poly(fluorenemethylene) systems. They confirmed that these compounds retain their cofacial conformations by ^{1}H NMR spectroscopy and X-ray crystallography. The first electron oxidation and photoelectron spectra of F1−F4 were also studied, and the results showed that polyfluorene donors F1−F4 do not undergo significant structural changes during (or soon after) electron detachment.[1,2] Effective overlap of π orbitals of fluorenes in the stack also provides electronic coupling between the subunits and facilitates electron and exciton transfer.[3,32] However, a detailed study of the electrochemistry of these compounds, and especially the nature of the subsequent electron transfer steps, has not appeared. Investigation of stepwise electron transfer in molecules with strongly interacting groups is often difficult within the available potential window of most solvents. Since these molecules also fluoresce, we also investigated their ECL.

In this work, we describe the electrochemistry, spectroscopy, and ECL of a novel set of π-stacked poly(fluorenemethylene) oligomers (F*n*, n = 1−6) in 1:1 acetonitrile/benzene (MeCN/Bz) solution. We evaluate the standard potentials of the successive removal of electrons from the fluorene species shown in Scheme 1, including the cases where one, two, three, or four electron waves were observed. Finally, ECL of F6 by generation of the radical cation in the presence of the coreactant oxalate is described along with the spectral characterization of the ECL emission.

EXPERIMENTAL SECTION

Materials. The synthesis of F1−F6 (Scheme 1) has been described previously.[2] Anhydrous acetonitrile (MeCN; 99.8%), anhydrous benzene (Bz; 99.8%), and anhydrous tetrahydrofuran (THF; 99.9%) were obtained from Sigma-Aldrich (St. Louis, MO) and transferred directly into an argon atmosphere glovebox (MBraun Inc., Stratham, NH) without further purification. Electrochemical grade tetra-*n*-butylammonium hexafluorophosphate ((TBA)PF_6) was dried in a vacuum oven at 100 °C prior to being transferred directly into the glovebox. Tetra-*n*-butylammonium oxalate (TBAOX) was prepared by mixing oxalic acid (6.3 g) and tetra-*n*-butylammonium hydroxide in water at a mole ratio of 1:2 followed by evaporation and drying in a rotary evaporator at room temperature for several days.[33]

UV−vis spectra were recorded using a 1 cm quartz cuvette on a Milton Roy Spectronic 3000 array spectrophotometer (Rochester, NY). Fluorescence spectra were recorded by using a Quanta Master spectrofluorimeter (Photon Technology International, Birmingham, NJ). UV−vis absorbance and fluorescence measurements were carried out in MeCN/Bz (1:1, v/v) solutions under air-saturated conditions. The relative fluorescence efficiencies were determined with respect to 9,10-diphenylanthracene (DPA) as a standard (λ_{ex} = 380 nm, Φ_{PL} = 0.91 in benzene).[34] An Agilent 6530 quadrupole time-of-flight (QTOF) mass spectrometer equipped with an atmospheric-pressure chemical ionization (APCI) source, and a Varian 12 T HiResMALDI Fourier transform ion cyclotron resonance (FT-ICR) system, and an Agilent 6530 equipped with an electrospray ionization (ESI) source, or a Thermo LTQ-XL ion trap system, were used for mass spectrum analysis.

dx.doi.org/10.1021/ja3057997 | J. Am. Chem. Soc. 2012, 134, 16265−16274

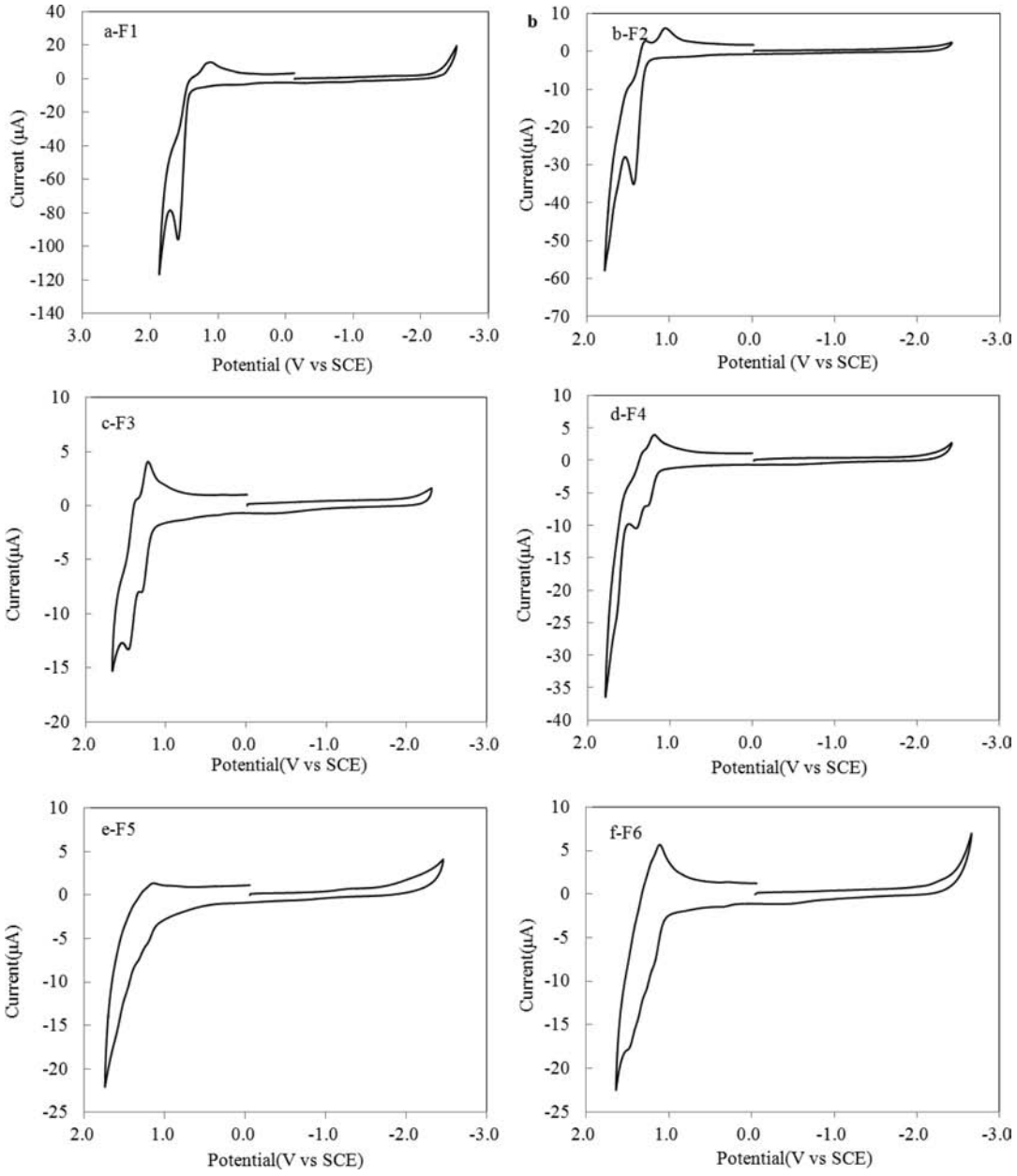

Figure 1. Cyclic voltammograms of (a) 2.5 mM monomer, (b) 1.3 mM dimer, (c) 0.7 mM trimer, (d) 0.3 mM tetramer, (e) 0.17 mM pentamer, and (f) 0.5 mM hexamer (scan rate 0.5 V/s, solvent 1:1 MeCN/Bz, supporting electrolyte 0.1 M $(TBA)PF_6$, platinum electrode area 0.043 cm^2).

MeCN/Bz (1:1, v/v) was used as the solvent and 0.1 M $(TBA)PF_6$ as the supporting electrolyte for all electrochemical investigations unless otherwise noted. All electrochemical experiments were done under anhydrous conditions. Electrochemical experiments were carried out using a three-electrode setup with a Pt disk working electrode (WE; $A = 0.043$ cm^2), a Pt wire counter electrode (CE), and a Ag wire quasi-reference electrode (RE). The Pt working electrode was bent at a 90° angle (L-type electrode) so that the electrode surface faced the detector in the ECL experiments. The working electrode was polished after each experiment with 0.3 μm alumina (Buehler, Ltd., Lake Bluff, IL) for several minutes, sonicated in water and in ethanol for 2 min, and dried in an oven at 120 °C. Potentials in CV were calibrated with ferrocene as an internal standard, taking its $E° = 0.342$ V vs SCE.[35] For chronoamperometry experiments, a 25 μm diameter Pt ultramicroelectrode (UME) was used as the working electrode. CV and chronoamperometry measurements were carried out with a CHI 660 electrochemical workstation (CH Instruments, Austin, TX). DigiSim 3.03 (Bioanalytical Systems, Inc., West Lafayette, IN) was used to simulate the cyclic voltammograms.

The geometric electrode area was determined by chronoamperometry using a 1 mM solution of ferrocene in MeCN and assuming a diffusion coefficient, D, of 1.2×10^{-5} cm^2/s. The diffusion coefficients of various poly(fluorenemethylene) oligomers were obtained from the observed scan rate dependences of the peak current on the basis of the Randles–Ševčik equation and from the chronoamperometric curve using the Cottrell equation.

The ECL transients and CV–ECL measurements were simultaneously recorded using an Autolab electrochemical workstation (Eco Chemie, The Netherlands) coupled with a photomultiplier tube (PMT; Hamamatsu R4220p, Japan) held at −750 V with a high-voltage power supply (Kepco, Flushing, NY). The photocurrent produced at the PMT was transformed into a voltage signal by an electrometer (Keithley 6517, Cleveland, OH), which was fed into the external input channel of an analog-to-digital converter (ADC) of the Autolab. ECL spectra were generated by using a CHI 660 electrochemical workstation and acquired with the Quanta Master spectrofluorimeter.

dx.doi.org/10.1021/ja3057997 | J. Am. Chem. Soc. 2012, 134, 16265–16274

Table 1. Electrochemical Results for Different Fluorenes

	$E_{1/2,ox1}$ (V), $A/A^{\bullet+}$	$E_{1/2,ox2}$ (V), $A^{\bullet+}/A^{\bullet2+}$	$E_{1/2,ox3}$ (V), $A^{\bullet2+}/A^{\bullet3+}$	$E_{1/2,ox4}$ (V), $A^{\bullet3+}/A^{\bullet4+}$	$D \times 10^5$ (cm^2/s)	$\Delta E_{1,2}$(V)	$\Delta E_{2,3}$(V)	$\Delta E_{3,4}$(V)
F1	1.65[a]				2.4			
F2	1.35[b]	1.58[b]			2.0	0.23		
F3	1.26[b]	1.43[b]			1.0	0.17		
F4	1.20[b]	1.34[b]	1.60[c]		0.8	0.14	0.26	
F5	1.19[c]	1.31[c]	1.45[c]		0.4	0.12	0.14	
F6	1.17[c]	1.24[c]	1.34[c]	1.45[c]	0.2	0.07	0.10	0.11

[a] $E_{1/2}$ values were obtained from the digital simulation. [b] $E_{1/2}$ values were obtained by averaging the cathodic and anodic peak potentials. [c] $E_{1/2}$ values were obtained by DPV or SWV.

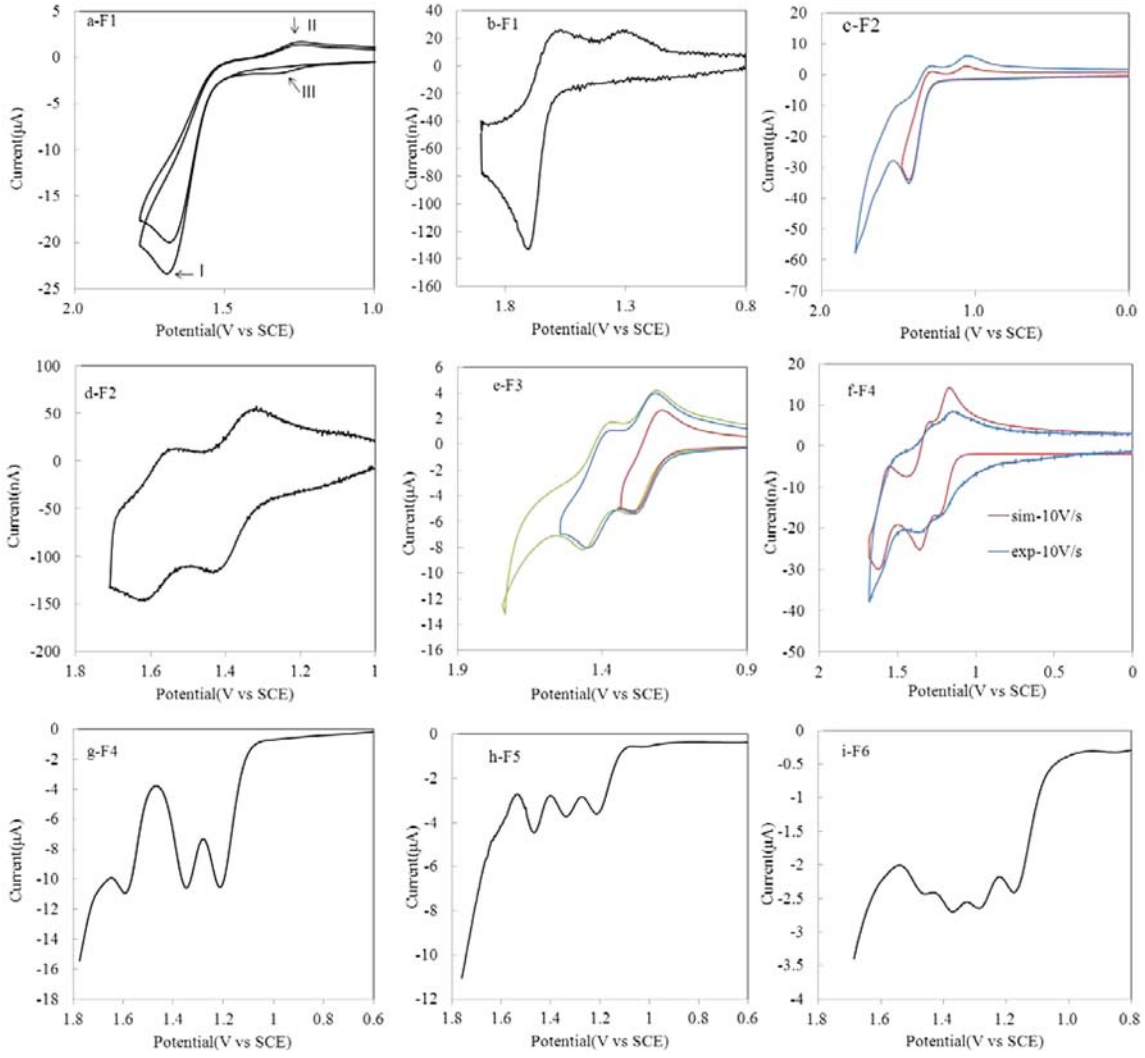

Figure 2. Continuous cyclic voltammogram of 0.72 mM monomer at 0.5 V/s (a). Cyclic voltammogram of 1.3 mM monomer at the Pt UME (r = 12.5 μm) with a 50 V/s scan rate (b). Cyclic voltammogram of 1.3 mM dimer at 0.5 V/s (c). Cyclic voltammogram of 1.1 mM dimer at the Pt UME (r = 12.5 μm) with a 50 V/s scan rate (d). Cyclic voltammogram of 0.5 mM trimer at 0.5 V/s at different potential ranges (e). Simulated and experimental oxidation waves for 0.5 mM tetramer at the UME (r = 12.5 μm) at 10 V/s (f). Square wave voltammogram of 0.8 mM tetramer (g). Differential pulse voltammogram for 0.3 mM pentamer (h). Square wave voltammogram of 0.3 mM hexamer (i) in 1:1 MeCN/Bz. The supporting electrolyte was 0.1 M $(TBA)PF_6$. A Pt electrode with an area of 0.043 cm^2 was used unless otherwise stated.

Bulk electrolysis was performed in a two-compartment cell. The compartments were separated by a fine-porosity glass frit. Mesh electrodes were used as the WE and CE. The RE was a silver wire. The WE and RE were placed in the same compartment with 2 mL of MeCN/Bz (1:1) containing 1 mM F6, 20 mM oxalate, and 0.1 M $(TBA)PF_6$. The CE compartment contained 2 mL of MeCN/Bz (1:1) and 0.1 M $(TBA)PF_6$. A magnetic stirring bar was used to maintain a uniform analyte concentration in the solution. A constant potential at 1.6 V vs Ag, the potential where maximum ECL was observed, was applied for 300 s, which was estimated to electrolyze about half of the F6 while ensuring minimal leakage between compartments. The potential was controlled using a CHI 660 electrochemical workstation.

RESULTS AND DISCUSSION

Electrochemistry. The potentials for the first oxidation wave of F1−F4 compounds have been reported in a preliminary study carried out in dichloromethane.[1] We describe

dx.doi.org/10.1021/ja3057997 | J. Am. Chem. Soc. 2012, 134, 16265−16274

here the electrochemical behavior of six compounds to study the interaction between the cofacially oriented fluorene moieties in these multiply stacked poly(fluorenemethylene) systems. Electrochemical measurements were carried out in MeCN/Bz (1:1, v/v) solution with 0.1 M (TBA)PF_6 as the supporting electrolyte unless stated otherwise. The cyclic voltammograms are shown in Figure 1. The half-wave potentials for the oxidation and the diffusion coefficients are summarized in Table 1. Fitting was carried out by subtraction of the background current and determining the best fit to the simulation (see Figures S2−S8 in the Supporting Information) corrected for the measured electrical double layer capacitance and the uncompensated cell resistance.

For F1, a first scan to positive potential at ν = 0.5 V/s, the anodic peak, corresponding to the 1e oxidation appeared at 1.69 V vs SCE. Upon scan reversal at this scan rate, no cathodic peaks corresponding to anodic peak I was seen, indicating that the radical cation is unstable. Instability upon oxidation can be ascribed in part to the absence of substituents, which is similar to that for small oligothiophenes.[27,36,37] However, cathodic peak II appeared on scan reversal at ca.1.25 V vs SCE, and in the second positive potential scan, a new associated anodic peak, III, was observed at ca. 1.34 V vs SCE (Figure 2a). The peak potential separation, II−III, was about 90 mV, suggesting a Nernstian redox response (with some uncompensated resistance). Upon repeated scans, the height of peak I decreased, while those of peaks II and III increased (Figure S1 in the Supporting Information). With increasing scan rate, for example, 30 V/s, the new reduction wave decreased and the reverse reduction wave can be observed, as seen in the cyclic voltammogram of F1 at the UME (Figure 2b).

Digital simulations were carried out for fast scan rate CV to determine the mechanism of the oxidation of F1 (Figure S2 in the Supporting Information). A reasonable fit was obtained for an ECE mechanism with formation of the radical cation followed by dimerization to produce a product that forms the reversible II/III couple, with a homogeneous dimerization forward rate constant, k_f, of about 4×10^4 M^{-1} s^{-1}. This can be compared to the 1e diphenylamine oxidation followed by the formation of the dimer, with a dimerization constant of 2×10^5 M^{-1} s^{-1}.[38]

F2 showed two irreversible 1e waves at a scan rate of 0.5 V/s (Figure 2c) but clearly showed two reversible 1e oxidation waves with half-wave potentials at +1.35 and +1.58 V vs SCE at faster scan rates (Figure 2d). A simple EE mechanism with two Nernstian electrochemical waves (Figure S3 in the Supporting Information) can be used in the digital simulation for fast scan rates. The potential of the first oxidation for F2 (1.35 V vs SCE) is less positive than that for F1, indicating an electronic interaction between the two fluorenes. This is consistent with the spectroscopic shift of F2 to longer wavelengths, as discussed below. The peak potential separation between the first and second oxidations, $\Delta E_{1,2}$, is 0.23 V. This splitting is consistent with a significant Coulombic repulsion between the two charged fluorene cations. The repulsive energy between the holes in the bonding orbitals of each fluorene moiety (0.23 V) is quite large compared with those of other compounds discussed below but is smaller than usually observed for organic compounds (0.5 V for aromatic hydrocarbons).[14]

F3 is characterized by the presence of two reversible waves with half-wave potentials of +1.26 and +1.43 V vs SCE on oxidation. As expected, it is harder to withdraw a third electron compared with the second one, so the third wave is shifted toward more positive potentials beyond the background oxidation in MeCN/Bz solution (Figure 2e and Supporting Information Figure S4). F3 shows a smaller separation between the first and second oxidation peaks ($\Delta E_{1,2}$ = 0.17 V) compared to F2 (0.23 V). F4 shows two reversible waves and one irreversible wave on oxidation at lower scan rate (<5 V/s, as shown in Figure 1d). At high scan rate, three reversible oxidation waves were observed (Figure 2f). It is more difficult to withdraw the fourth electron compared with the third one, and this wave was not seen in MeCN/Bz solution. The oxidation half-wave potentials for F4 are at +1.20, 1.34, and +1.60 V vs SCE, as obtained from CV and digital simulations assuming an EEE mechanism with three Nernstian waves (Figures S5 and S6 in the Supporting Information). The cyclic voltammograms for the larger oligomers are not very good because the low solubility allows only low concentrations (<0.8 mM) so that they were distorted significantly by the background and capacitive currents. Moreover, as discussed later, there is evidence for additional reactions of the radical cation and more highly oxidized species. Since we are mainly interested in the potentials of the waves, the agreement, though poor, should be sufficient.

To obtain better resolution of the waves, square wave voltammetry (SWV), which produces peak-shaped waves, was also employed (Figure 2g). For F4, $\Delta E_{1,2}$ = 0.14 V, compared to 0.17 V for F3 and 0.23 V for F2. $\Delta E_{2,3}$ = 0.18 V, which is larger than $\Delta E_{1,2}$.

F5 also shows three reversible waves on oxidation, with half-wave potentials of +1.19, +1.31, and +1.45 V vs SCE, as obtained from differential pulse voltammetry (DPV), which produces peak-shaped waves (Figure 2h). Simple digital simulations assuming an EEE mechanism with three Nernstian waves (Figure S7 in the Supporting Information) were used to further confirm three electron transfers. For F5, $\Delta E_{1,2}$ = 0.12 V is smaller than $\Delta E_{1,2}$ for the smaller oligomers. Similarly, $\Delta E_{2,3}$ = 0.14 V < $\Delta E_{2,3}$ for F4.

F6 shows four reversible waves (Figures 1f and 2i) with half-wave potentials of +1.17, 1.24, 1.34, and +1.45 V vs SCE. Better resolution was obtained with SWV (Figure 2i). Digital simulations assume an EEEE mechanism with four Nernstian waves (Supporting Information Figure S8), in which the potentials are in agreement with those from experimental data. For F6, $\Delta E_{1,2}$ = 0.07 V is smaller than $\Delta E_{1,2}$ of F2 to F5 (Table 1). Moreover, for F6, $\Delta E_{2,3}$ = 0.10 V is smaller than that for F4 and F5. For F6, the $\Delta E_{3,4}$ of 0.11 V seems surprisingly small.

No well-defined reduction peaks were observed up to around −2.4 V vs SCE in the MeCN/Bz solution. THF, which has a more negative working potential range, also gave no well-defined CV reduction peaks except for some broad shoulders at ∼−3.2 V vs SCE (Figure S9 in the Supporting Information). From the spectroscopy of these compounds, shown below, the difference in energy between the highest occupied molecular orbital (HOMO) and lowest unoccupied molecular orbital (LUMO) is ∼3.5 eV (∼350 nm), which would put the potentials for reduction in MeCN/Bz beyond ∼−2.3 V.

Correlation of Electrochemical Potentials. The dependence of the electrochemical potential on $1/n$, where n = 1−6 is the number of repeating units, is shown in Figure 3. In all cases the oxidation peak potential decreased with an increasing number of fluorene moieties. In other words, the removal of the first electron from a fluorene moiety becomes easier as n increases. Moreover, as previously reported for F1 through F4,[1] the oxidation half-wave potential values are not linear with n for

dx.doi.org/10.1021/ja3057997 | J. Am. Chem. Soc. 2012, 134, 16265−16274

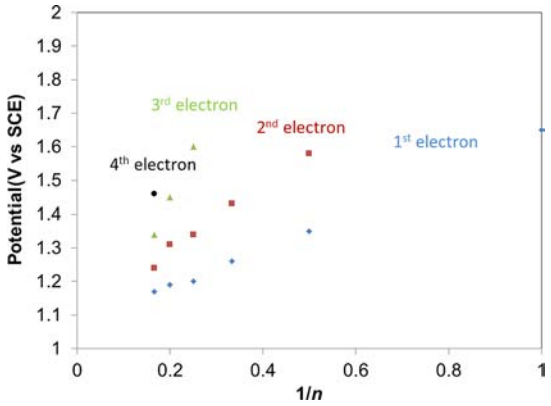

Figure 3. Dependence of the oxidation potential on $1/n$ for poly(fluorenemethylene) oligomers. The colored symbols are correlated with the removal of consecutive electrons: blue tilted squares (first electron), red squares (second electron), green triangles (third electron), black circles (fourth electron); n = 1, 2, 3, 4, 5, and 6 correspond to F1, F2, F3, F4, F5, and F6.

F1−F6, but rather with $1/n$. For F1, the absence of substituents allows nucleophilic attack, resulting in the instability of the radical cation. This following homogeneous reaction (an EC scheme) causes the apparent half-wave potential to be less positive than the thermodynamic $E_{1/2,ox1}$, accounting for the apparent deviation from the fairly linear behavior of the behavior of F2−F6 in Figure 3. For F2−F6, which show Nernstian first waves, the potentials correspond to thermodynamic values. This change in $E_{1/2,ox1}$ demonstrates considerable delocalization of the charge with increasing n. The slope of the $E_{1/2,ox1}$ vs $1/n$ plot for F2−F6 is 0.55 V, which is much smaller than that for thiophene oligomers (2.33 V).[39]

The second and successive peaks reflect interactions between charges on different monomer units. This potential difference, $\Delta E_{1,2}$, correlates with the size of the oligomer, since the electrostatic interactions between the two positive charges decreases the further apart they are (i.e., with increasing distance).[13,40] It is more difficult (i.e., a larger ΔE) to remove the third or fourth electron compared to the second, as seen, for example, in the larger $\Delta E_{2,3}$ separations for F4, F5, and F6 as compared with the corresponding $\Delta E_{1,2}$ values as shown in Table 1. For example, F4 shows a smaller separation ($\Delta E_{1,2}$ = 0.14 V) between the first and second oxidation peaks compared with that of $\Delta E_{2,3}$ (0.26 V). Removing a third electron is energetically much more difficult because of Coulombic repulsive forces.

Although the trend of the first electron removal with oligomer size shows the effects of considerable delocalization of charge, a simple localized scheme can be used to predict the relative spacing between successive electron transfers, as suggested in Scheme 2. For example, according to Coulomb's law, the energy for the removal of the second electron based on electrostatic interactions, assuming the second charge locates at the other end of the oligomer, can be taken as

$$U_{1,2} = \mathrm{cnst_a}(q_1 q_2 / r_{1,2}) = \mathrm{cnst_b}(1/(n-1)) \quad (1)$$

where $\mathrm{cnst_a} = 1/4\pi\varepsilon$, $q_2 = q_1 = e$, the electronic charge, and $r_{1,2}$ = the distance between the charges, taken as $(n-1)d$, where d is the distance between fluorene units; $\mathrm{cnst_b}$ contains the factors e and d. A plot of $\Delta E_{1,2}$ (assumed to be proportional to $U_{1,2}$) vs $1/(n-1)$ is linear (Figure 4a). Similarly for the removal of the third electron, the energy of three charges is given by

Scheme 2. Illustration of Multiple, Interacting Electron Transfers in π-Stacked Poly(fluorenemethylene) Oligomers, Where $r_{12} = 5d$, $r_{13} = 2d$, $r_{23} = 3d$, and $r_{3,4} = 2d$

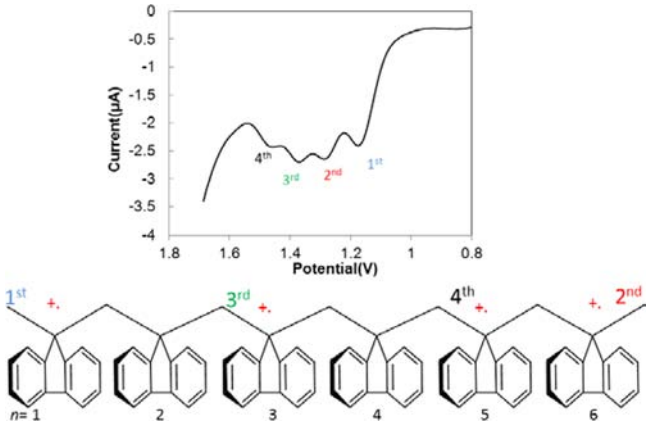

$$U_{2,3} = \mathrm{cnst_a}(q_1 q_2 / r_{12} + q_1 q_3 / r_{13} + q_2 q_3 / r_{23}) \quad (2)$$

Again q is equal to e and r_{13}, r_{12}, and r_{23} are taken for a given oligomer to minimize the electrostatic interaction. For example, for F4, $r_{13} = d$, $r_{12} = 3d$, and $r_{23} = 2d$. For F6, as shown in Scheme 2, $r_{12} = 5d$, $r_{13} = 2d$, $r_{23} = 3d$, and $r_{3,4} = 2d$ (1, 2, 3, and 4 correspond to first electron, second electron, third electron, and fourth electron).

This yields

$$\Delta U_{2,3} \propto \mathrm{cnst_a}(1/r_{12} + 1/r_{13} + 1/r_{23}) \quad (3)$$

resulting in the plot in Figure 4b.

We also observed multielectron transfer behavior with thiophene and fluorene oligomers.[39] We used the above-mentioned simple localized scheme to predict the relative spacing between successive electron transfers of these as well as shown in Figure 4c−f. A good fit was obtained for both thiophene and fluorene. The difference between the slopes may be ascribed to the electronic delocalization on these compounds. A small slope was also observed for poly(fluorenemethylene) oligomers compared with t-thiophene and f-fluorene.

Moreover, scan rate studies showed that the peak currents of the oxidation wave ($i_{p,o}$) increased linearly with the square root of the scan rate ($\nu^{1/2}$) for the oxidation, indicating diffusion control of the current (Figure 5). The diffusion coefficient, D, is found by plotting $i_{p,o}$ vs $\nu^{1/2}$ and is listed in Table 1, assuming the first oxidation wave involved a single electron transfer step. To confirm this n = 1 assumption, chronoamperometry at a Pt UME was carried out to determine the number of electrons (n) and diffusion coefficient independent of the concentration.[41] The D value found from the current transient agreed with that from CV, which confirmed the n = 1 nature of the oxidation wave (Figure S10 in the Supporting Information).

Summarizing this section, it can be seen that there are multiple discrete electron transfers observable in the π-stacked poly(fluorenemethylene) oligomers, unlike the results with poly(2-vinylnaphthalene), poly(9-vinylanthracene),[11] and poly(vinylferrocene).[6] Moreover, the interactions between the electroactive fluorene moieties are reflected by the potential difference between peaks and are dependent on electrostatic interactions, distance, and electronic delocalization on these compounds.

dx.doi.org/10.1021/ja3057997 | J. Am. Chem. Soc. 2012, 134, 16265−16274

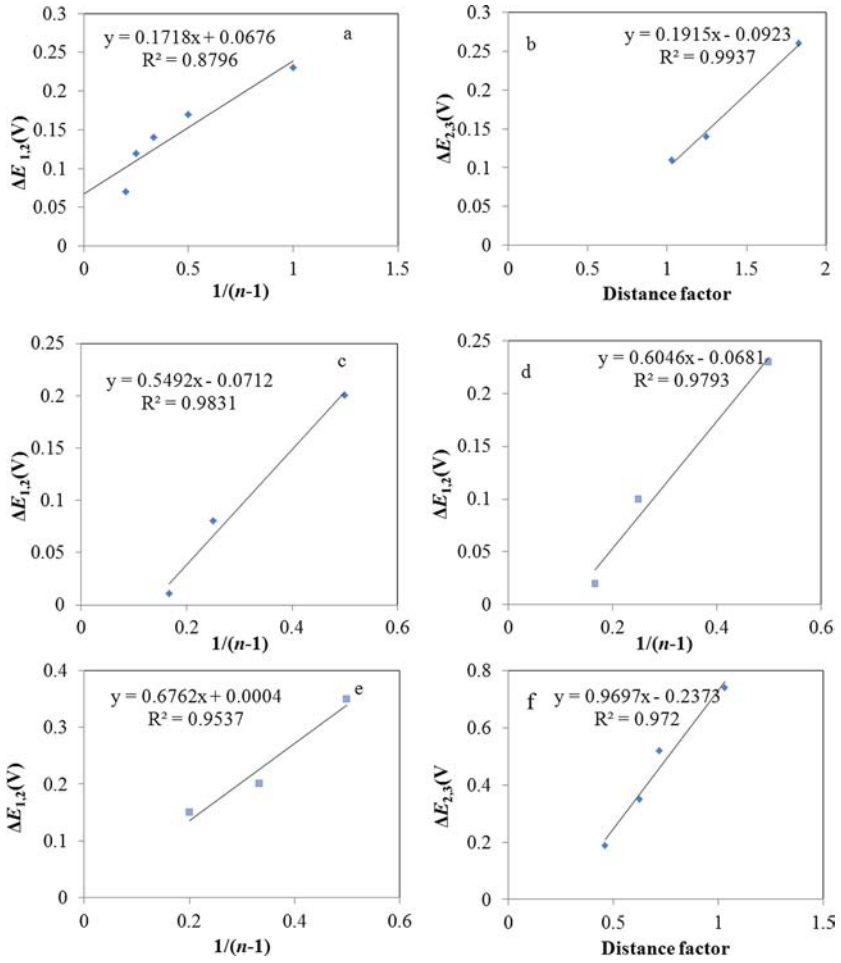

Figure 4. $\Delta E_{1,2}$ vs $1/(n-1)$ for poly(fluorenemethylene) oligomer oxidation (a). $\Delta E_{2,3}$ vs distance factor for poly(fluorenemethylene) oligomer oxidation (b). $\Delta E_{1,2}$ vs $1/(n-1)$ for f-fluorene oxidation (c). $\Delta E_{1,2}$ vs $1/(n-1)$ for f-fluorene reduction (d). $\Delta E_{1,2}$ vs $1/(n-1)$ for t-thiophene reduction (e). $\Delta E_{2,3}$ vs distance factor for t-thiophene reduction (f). Data for (c)−(f) are from ref 39.

Spectroscopy. The normalized UV−vis absorption and fluorescence (photoluminescence, PL) spectra for F1−F6 are shown in Figures 6 and 7, which were obtained in the same solvent as that used for the electrochemical measurement. The optical properties, absorption and emission maxima, fluorescence quantum yield, and optical energy gap are summarized in Table 2. For the monomer, a maximum absorption peak at 302 nm and a maximum emission peak at 316 nm were observed, while a maximum absorption peak at 304 nm and a maximum emission peak at 394 nm were observed for the dimer. The large red shifts for the adsorption and emission from monomer to oligomers is consistent with the electrochemical evidence of electronic delocalization in these poly(fluorenemethylene) oligomers.

Compared to F2, much smaller red shifts of ∼1 nm are found for F3−F6.[42] No exciton splitting was observed for the six fluorenes, consistent with the small peak potential separation.[7] The PL quantum yields (Φ_{FL}) for F1−F6 were determined in a MeCN/Bz solution with DPA as the standard (φ_{fluor} = 0.91 in benzene), and the results are shown in Table 2. The molar absorption coefficient ε increased and the fluorescence quantum yield, φ_{fluor}, decreased slightly with n. This would suggest that the backbone geometry changes significantly on going from the ground state (S0) to the vibronically relaxed excited state (S1).[43]

Electrogenerated Chemiluminescence. Because of the extreme negative reduction potentials of these compounds, annihilation ECL could not be generated; i.e., no solvent was found suitable for both the oxidation and reduction of these. However, coreactant ECL tied to the oxidation was possible, and TBAOX was used as a coreactant to form the needed reductant, $CO_2^{\bullet-}$. In this work we only report the ECL of F6 in the presence of $C_2O_4^{2-}$. The other compounds also showed ECL that was significantly weaker than F6, so it was not possible to obtain their ECL spectra. The oxidation of $C_2O_4^{2-}$ produces $CO_2^{\bullet-}$ (eq 4). This species is a strong reducing agent (E° = −2.2 V vs SCE)[33] and can react with the F6 radical cation to produce the excited state.

$$C_2O_4^{2-} - e \rightarrow CO_2 + CO_2^{\bullet-} \quad (4)$$

The results of an ECL experiment with 0.5 mM F6 and 20 mM tetra-*n*-butylammonium oxalate in MeCN/Bz (1:1) containing 0.1 M (TBA)PF_6 at a Pt electrode is shown in Figure 8. No ECL was seen on oxidation when either F6 or TBAOX was absent from the test solution. The addition of oxalate causes the oxidation current of F6 to increase sharply while the reversal peak disappears as expected for a catalytic reaction (EC') wave.[33] A strong ECL signal appeared at the potential for the oxidation of F6. The enthalpy was calculated from the first oxidation potential of F6 (1.17 V vs SCE) and the reduction potential of $CO_2^{\bullet-}$ (E° = −2.2 V vs SCE) by the

dx.doi.org/10.1021/ja3057997 | J. Am. Chem. Soc. 2012, 134, 16265−16274

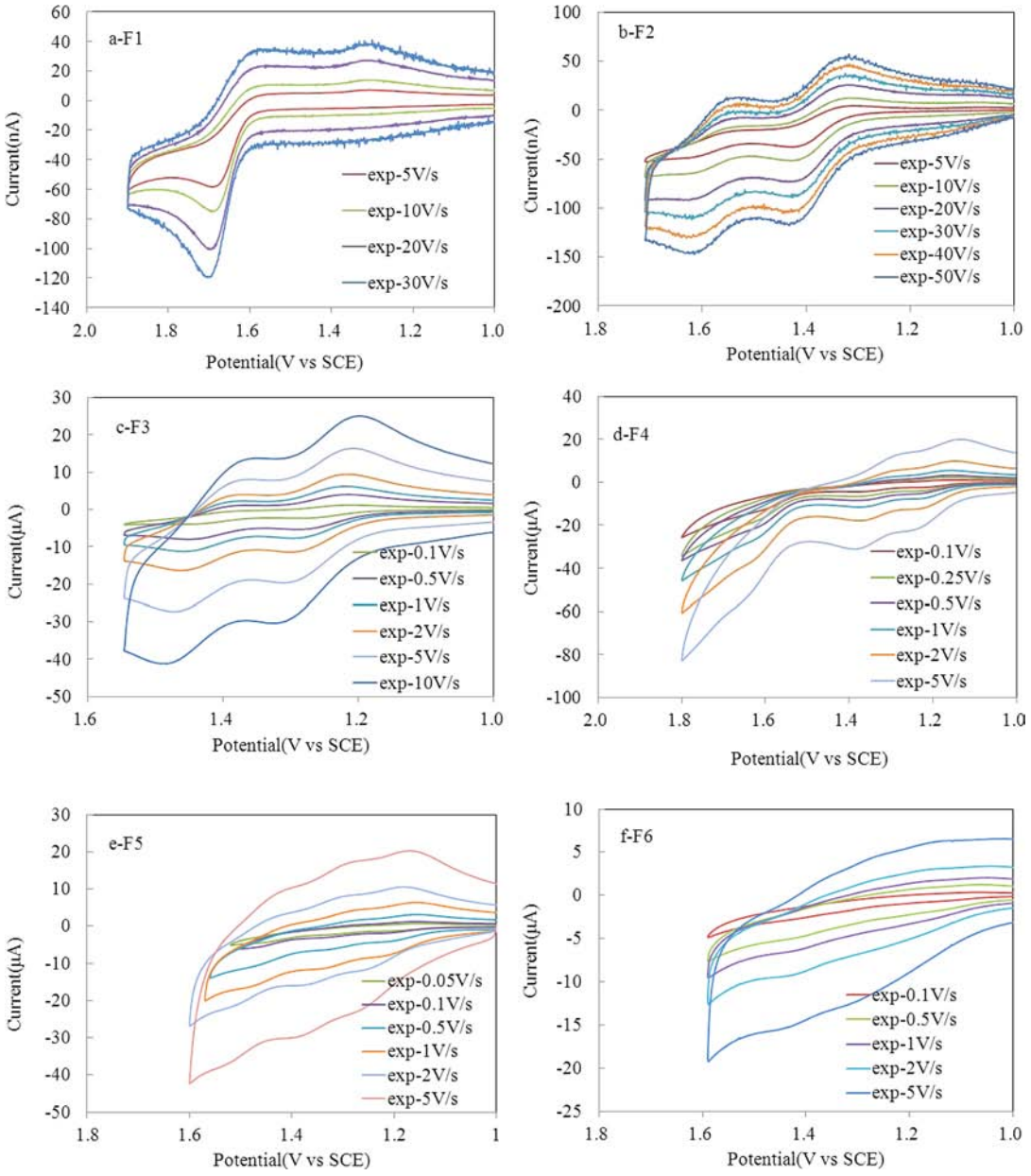

Figure 5. Scan rate dependence of cyclic voltammograms for poly(fluorenemethylene) oligomers: 1.3 mM monomer (a) and 1.1 mM dimer (b) at the Pt UME with r = 12.5 μm and 0.5 mM trimer (c), 0.3 mM tetramer (d), 0.4 mM pentamer (e), and 0.2 mM hexamer (f) at the Pt electrode with a 0.043 cm^2 area. Experimental conditions: solvent 1:1 MeCN/Bz, supporting electrolyte 0.1 M (TBA)PF_6.

equation $-\Delta H_{co} = -\Delta G_{co} - T\Delta S$ with the entropy term ($T\Delta S$) estimated as 0.1 eV.[44] This is larger than the energy for the excited singlet state, E_s = 3.13 eV, suggesting direct formation of the singlet is possible. However, only longer wavelength emission at 550 nm was predominant with negligible ECL at 395 nm, where the fluorescence emission was observed for F6 (Figure 8b). Often the presence of ECL emission at wavelengths longer than the fluorescence is ascribed to excimer emission. However, in that case there is no long-wavelength emission in the presence of a coreactant because in this case direct formation of an excimer by annihilation of the radical anion and cation does not occur directly.[45,46] Thus, the long-wavelength emission at 550 nm in the presence of a coreactant we observe here (Figure 8b) is more likely from a byproduct from reaction of the electrogenerated radical cation.

To test this hypothesis, bulk electrolysis was performed in 1 mM F6 in the presence of 20 mM oxalate and 0.1 M (TBA)PF_6. The current−time data were recorded during the experiment (as shown in Figure S11 in the Supporting Information). After bulk electrolysis, the solution in the first compartment cell was gathered, and the mass spectrum, UV−vis spectrum, and fluorescence spectrum were measured (Figures S12 and S13 in the Supporting Information). After oxidation bulk electrolysis at +1.6 V vs Ag (MeCN:Bz) for 300 s, a new small absorption peak was observed at 360 nm (Figure S12 in the Supporting Information) and longer wavelength PL emission at a wavelength similar to that of the peak of the ECL spectrum was observed at 550 nm (Figure S13 in the Supporting Information). This emission is perhaps the result of byproduct from the reaction of the electrogenerated radical cation, but attempts to identify the product by mass

dx.doi.org/10.1021/ja3057997 | J. Am. Chem. Soc. 2012, 134, 16265−16274

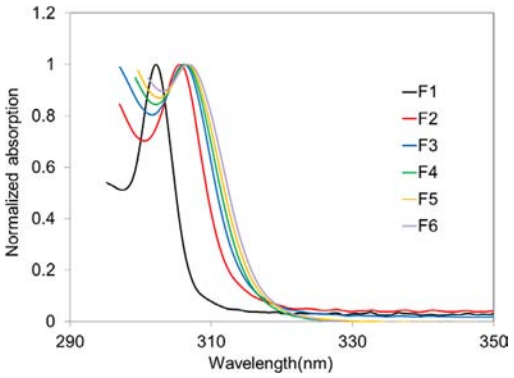

Figure 6. Normalized absorption spectra for the monomer (black line), dimer (red line), trimer (blue line), tetramer (green line), pentamer (orange line), and hexamer (purple line).

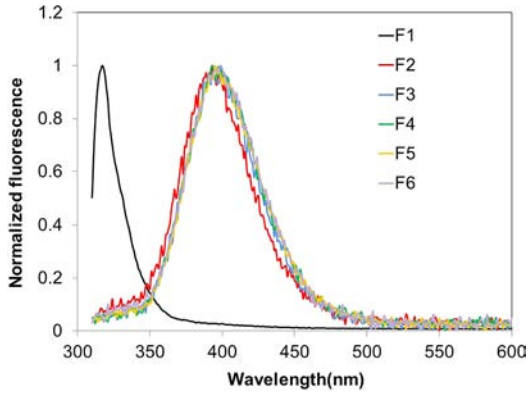

Figure 7. Normalized fluorescence spectra for the monomer (black line), dimer (red line), trimer (blue line), tetramer (green line), pentamer (orange line), and hexamer (purple line). The excitation wavelength for the monomer was 302 nm, that for the dimer was 305 nm, and that for the other fluorenes was 306 nm.

Table 2. Photophysical Properties of Different Poly(fluorenemethylene) Oligomers

dye	λ_{max}(abs) (nm)	ε (M^{-1} cm^{-1})	λ_{max}(fluor) (nm)	φ_{fluor}	E_s[a] (eV)
monomer	302	3.3×10^3	315	0.34	3.93
dimer	305	4.3×10^3	394	0.15	3.14
trimer	306	4.8×10^3	395	0.11	3.13
tetramer	306	7.1×10^3	395	0.081	3.13
pentamer	306	14.1×10^3	395	0.085	3.13
hexamer	306	13.9×10^3	395	0.11	3.13

[a] E_s is the approximate energy of the singlet state taken as the fluorescence wavelength maximum, $E_s = 1239.81/\lambda_{max}$(FL) (nm).

spectrometry were not successful (see Supporting Information Figures S14–S16). A clear explanation for the long-wavelength emission is still a challenge, and the ECL nature of the byproduct is still an open question.

In addition, pulsing between 0 and +1.60 V produced strong ECL emission. As expected, light was generated at the oxidation potential of 1.6 V vs Ag with no ECL seen when the electrode potential was stepped back to 0.0 V. Within a pulse the ECL intensity decayed more slowly compared to the usual mass transfer controlled annihilation (Figure S17, Supporting Information).[45] The slow decay is a function of the kinetics of the chemical reaction of the electrogenerated radical cation and oxalate ion. The situation is complicated because of the additional occurrence of a side reaction of the radical cation producing the long-wavelength-emitting product.

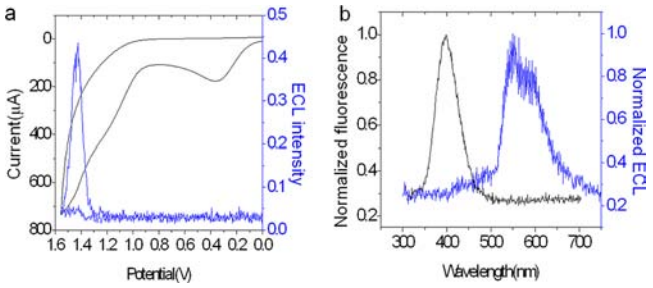

Figure 8. (a) ECL (blue line)–CV (black line) simultaneous measurements for 0.5 mM F6 in the presence of 20 mM $C_2O_4^{2-}$. (b) ECL (blue line) and fluorescence (black line) spectra for 0.5 mM F6 in the presence of 20 mM $C_2O_4^{2-}$. Spectra were generated by pulsing the potential from 0 to +1.60 V versus Ag. The Pt electrode area was 0.043 cm^2 in MeCN/Bz (1:1) containing 0.1 M (TBA)PF_6.

CONCLUSIONS

We have studied the electrochemistry, spectroscopy, and ECL behaviors of six π-stacked poly(fluorenemethylene) oligomers. All compounds gave a multiple, interacting one electron transfer oxidation. The addition of the first electron to a fluorene oligomer became easier as the number of fluorene units increased, and this addition was correlated with the distance between fluorene moieties and the electrostatic repulsive interaction with the extent of conjugation. No well-defined reduction peaks were observed except for some broad signals at around −3.2 V vs SCE in THF. No characteristic annihilation ECL signal was obtained for the samples, while ECL emission was observed in the presence of $C_2O_4^{2-}$. A long-wavelength ECL emission resulting from a reaction product based on fluorescence following bulk electrolysis is proposed. This work demonstrates the interactions between aromatic rings via π-stacking by van der Waals forces, which can provide some information for the future design of next-generation conducting wirelike materials for practical applications in the emerging field of nanotechnology.

ASSOCIATED CONTENT

Supporting Information

Simulated and experimental CVs, UV–vis spectra, fluorescence spectra, and mass spectra. This material is available free of charge via the Internet at http://pubs.acs.org.

AUTHOR INFORMATION

Corresponding Author

ajbard@mail.utexas.edu

Notes

The authors declare no competing financial interest.

ACKNOWLEDGMENTS

We acknowledge support from the Robert A. Welch Foundation (Grant F-0021) and the National Science Foundation (Grant CHE-1111518). H. L. Qi thanks the National Natural Science Foundation of China (Grants 20805028 and 21027007) and the National Scholarship Fund of China Scholarship Council (Grant 2010687526) for support. We also thank Dr. Fu-Ren F. Fan for valuable discussion and

Dr. Alexander B. Nepomnyashchii and Dr. Jungdon Suk for primary study of these compounds.

REFERENCES

(1) Rathore, R.; Abdelwahed, S. H.; Guzei, I. A. *J. Am. Chem. Soc.* **2003**, *125*, 8712.
(2) Rathore, R.; Abdelwahed, S. H.; Kiesewetter, M. K.; Reiter, R. C.; Stevenson, C. D. *J. Phys. Chem. B* **2006**, *110*, 1536.
(3) Vura-Weis, J.; Abdelwahed, S. H.; Shukla, R.; Rathore, R.; Ratner, M. A.; Wasielewski, M. R. *Science* **2010**, *328*, 1547.
(4) Evans, D. H. *Chem. Rev.* **2008**, *108*, 2113.
(5) Astruc, D.; Boisselier, E.; Ornelas, C. *Chem. Rev.* **2010**, *110*, 1857.
(6) Flanagan, J. B.; Margel, S.; Bard, A. J.; Anson, F. C. *J. Am. Chem. Soc.* **1978**, *100*, 4248.
(7) Nepomnyashchii, A. B.; Bard, A. J. *Acc. Chem. Res.* **2012**, DOI: 10.1021/ar200278b.
(8) Nepomnyashchii, A. B.; Broring, M.; Ahrens, J.; Bard, A. J. *J. Am. Chem. Soc.* **2011**, *133*, 8633.
(9) Nepomnyashchii, A. B.; Broring, M.; Ahrens, J.; Bard, A. J. *J. Am. Chem. Soc.* **2011**, *133*, 19498.
(10) Rosenthal, J.; Nepomnyashchii, A. B.; Kozhukh, J.; Bard, A. J.; Lippard, S. J. *J. Phys. Chem. C* **2011**, *115*, 17993.
(11) Saji, T.; Pasch, N. F.; Webber, S. E.; Bard, A. J. *J. Phys. Chem.* **1978**, *82*, 1101.
(12) Ammar, F.; Saveant, J. M. *J. Electroanal. Chem.* **1973**, *47*, 115.
(13) Itaya, K.; Bard, A. J.; Szwarc, M. *Z. Phys. Chem., Neue Folge* **1978**, *112*, 1.
(14) Suk, J.; Natarajan, P.; Moorthy, J. N.; Bard, A. J. *J. Am. Chem. Soc.* **2012**, *134*, 3451.
(15) Fry, A. J. *Electrochem. Commun.* **2005**, *7*, 602.
(16) Wopschal., Rh; Shain, I. *Anal. Chem.* **1967**, *39*, 1514.
(17) Hapiot, P. F.; Kispert, L. D.; Konovalov, V. V.; Saveant, J. M. *J. Am. Chem. Soc.* **2001**, *123*, 6669.
(18) Nepomnyashchii, A. B.; Broring, M.; Ahrens, J.; Kruger, R.; Bard, A. J. *J. Phys. Chem. C* **2010**, *114*, 14453.
(19) Nepomnyashchii, A. B.; Broring, M.; Ahrens, J.; Bard, A. J. *J. Am. Chem. Soc.* **2011**, *133*, 8633.
(20) Smith, T. W.; Kuder, J. E.; Wychick, D. *J. Polym. Sci., Polym. Chem.* **1976**, *14*, 2433.
(21) Myers, R. L.; Shain, I. *Anal. Chem.* **1969**, *41*, 980.
(22) Macias-Ruvalcaba, N. A.; Evans, D. H. *J. Phys. Chem. B* **2006**, *110*, 5155.
(23) Omer, K. M.; Kanibolotsky, A. L.; Skabara, P. J.; Perepichka, I. F.; Bard, A. J. *J. Phys. Chem. B* **2007**, *111*, 6612.
(24) Omer, K. M.; Ku, S. Y.; Wong, K. T.; Bard, A. J. *Angew. Chem., Int. Ed.* **2009**, *48*, 9300.
(25) Wong, K. T.; Chen, Y. M.; Lin, Y. T.; Su, H. C.; Wu, C. C. *Org. Lett.* **2005**, *7*, 5361.
(26) Wong, K. T.; Liao, Y. L.; Lin, Y. T.; Su, H. C.; Wu, C. C. *Org. Lett.* **2005**, *7*, 5131.
(27) Choi, J. P.; Wong, K. T.; Chen, Y. M.; Yu, J. K.; Chou, P. T.; Bard, A. J. *J. Phys. Chem. B* **2003**, *107*, 14407.
(28) Fungo, F.; Wong, K. T.; Ku, S. Y.; Hung, Y. Y.; Bard, A. J. *J. Phys. Chem. B* **2005**, *109*, 3984.
(29) Rashidnadimi, S.; Hung, T. H.; Wong, K. T.; Bard, A. J. *J. Am. Chem. Soc.* **2008**, *130*, 634.
(30) Omer, K. M.; Ku, S. Y.; Wong, K. T.; Bard, A. J. *J. Am. Chem. Soc.* **2009**, *131*, 10733.
(31) Wartini, A. R.; Staab, H. A.; Neugebauer, F. A. *Eur. J. Org. Chem.* **1998**, 1161.
(32) Voityuk, A. A. *J. Phys. Chem. C* **2010**, *114*, 20236.
(33) Chang, M. M.; Saji, T.; Bard, A. J. *J. Am. Chem. Soc.* **1977**, *99*, 5399.
(34) Stevens, B.; Algar, B. E. *J. Phys. Chem.* **1968**, *72*, 2582.
(35) Sahami, S.; Weaver, M. J. *J. Electroanal. Chem.* **1981**, *122*, 155.
(36) Hill, M. G.; Penneau, J. F.; Zinger, B.; Mann, K. R.; Miller, L. L. *Chem. Mater.* **1992**, *4*, 1106.
(37) Becker, R. S.; deMelo, J. S.; Macanita, A. L.; Elisei, F. *J. Phys. Chem.* **1996**, *100*, 18683.
(38) Yang, H. G.; Bard, A. J. *J. Electroanal. Chem.* **1991**, *306*, 87.
(39) Nepomnyashchii, A. B.; Ono, R. J.; Lyons, D. M.; Bielawski, C. W.; Sessler, J. L.; Bard, A. J. *Chem. Sci.* **2012**, *3*, 2628.
(40) Macias-Ruvalcaba, N. A.; Telo, J. P.; Evans, D. H. *J. Electroanal. Chem.* **2007**, *600*, 294.
(41) Denuault, G.; Mirkin, M. V.; Bard, A. J. *J. Electroanal. Chem.* **1991**, *308*, 27.
(42) Anemian, R.; Mulatier, J. C.; Andraud, C.; Stephan, O.; Vial, J. C. *Chem. Commun.* **2002**, 1608.
(43) Klaerner, G.; Miller, R. D. *Macromolecules* **1998**, *31*, 2007.
(44) Choi, J. P.; Bard, A. J. *J. Electroanal. Chem.* **2004**, *573*, 215.
(45) Miao, W. J. *Chem. Rev.* **2008**, *108*, 2506.
(46) Bard, A. J. *Electrogenerated Chemiluminescence*; Marcel Dekker: New York, 2004.